ELSEVIER

Composites Science and Technology 62 (2002) 1869–1880

COMPOSITES SCIENCE AND TECHNOLOGY

www.elsevier.com/locate/compscitech

Equivalent-continuum modeling of nano-structured materials

Gregory M. Odegard[a,*], Thomas S. Gates[b], Lee M. Nicholson[c], Kristopher E. Wise[d]

[a]*National Research Council, NASA Langley Research Center, MS 188E, Hampton, VA 23681, USA*
[b]*NASA Langley Research Center, MS 188E, Hampton, VA 23681, USA*
[c]*ICASE, NASA Langley Research Center, MS 188E, Hampton, VA 23681, USA*
[d]*National Research Council, NASA Langley Research Center, MS 226, Hampton, VA 23681, USA*

Received 11 January 2002; received in revised form 12 June 2002; accepted 13 June 2002

Abstract

A method has been proposed for developing structure-property relationships of nano-structured materials. This method serves as a link between computational chemistry and solid mechanics by substituting discrete molecular structures with equivalent-continuum models. It has been shown that this substitution may be accomplished by equating the molecular potential energy of a nano-structured material with the strain energy of representative truss and continuum models. As important examples with direct application to the development and characterization of single-walled carbon nanotubes and the design of nanotube-based structural devices, the modeling technique has been applied to two independent examples: the determination of the effective-continuum geometry and bending rigidity of a graphene sheet. A representative volume element of the chemical structure of graphene has been substituted with equivalent-truss and equivalent-continuum models. As a result, an effective thickness of the continuum model has been determined. The determined effective thickness is significantly larger than the inter-planar spacing of graphite. The effective bending rigidity of the equivalent-continuum model of a graphene sheet was determined by equating the molecular potential energy of the molecular model of a graphene sheet subjected to cylindrical bending (to form a nanotube) with the strain energy of an equivalent-continuum plate subjected to cylindrical bending.

Keywords: Nanotechnology

1. Introduction

Nano-structured materials have generated considerable interest in the materials research community in the last few years partly due to their potentially remarkable mechanical properties [1]. In particular, materials such as carbon nanotubes, nanotube and nanoparticle-reinforced polymers and metals, and nano-layered materials have shown considerable promise. For example, carbon nanotubes could potentially have a Young's modulus as high as 1 TPa and a tensile strength approaching 100 GPa. The design and fabrication of these materials are performed on the nanometer scale with the ultimate goal to obtain highly desirable macroscopic properties.

One of the fundamental issues that needs to be addressed in modeling macroscopic mechanical behavior of nano-structured materials based on molecular structure is the large difference in length scales. On the opposite ends of the length scale spectrum are computational chemistry and solid mechanics, each of which consists of highly developed and reliable modeling methods. Computational chemistry models predict molecular properties based on known quantum interactions, and computational solid mechanics models predict the macroscopic mechanical behavior of materials idealized as continuous media based on known bulk material properties. However, a corresponding model does not exist in the intermediate length scale range. If a hierarchical approach is used to model the macroscopic behavior of nano-structured materials, then a methodology must be developed to link the molecular structure and macroscopic properties.

In this paper, a methodology for linking computational chemistry and solid mechanics models has been developed. This tool allows molecular properties of nano-structured materials obtained through molecular mechanics models to be used directly in determining the

* Corresponding author. Tel.: +1-757-864-2759.
E-mail address: g.m.odegard@larc.nasa.gov (G.M. Odegard).

0266-3538/02/$ - see front matter
PII: S0266-3538(02)00113-6

Nomenclature

Molecular model and force field

E^{el}	Non-bonded electrostatic potential energy
E^{g}	Molecular potential energy of graphene sheet
E^{nsm}	Potential energy of nano-structured material
E^{vdW}	Non-bonded van der Waals potential energy
E^{ϑ}	Bond-angle variation potential energy
E^{ρ}	Bond stretching potential energy
E^{τ}	Bond torsion potential energy
E^{ω}	Bond inversion potential energy
K_m^{ρ}	Force constant associated with the stretching of bond m
K_m^{θ}	Force constant associated with angle variation of bond angle m
K^{ω}	Force constant associated with bond inversion
$\overline{K^{\omega}}$	Modified force constant associated with bond inversion
L	Length of carbon nanotube
N	Number of atoms per carbon nanotube
p	Total number of carbon atoms in carbon structure
α	Interatomic spacing of carbon atoms in graphite
r^{nt}	Radius of carbon nanotube
$\bar{\phi}_p$	Average inversion angle (radians)
$\phi_{\sigma\pi}$	Angle between σ and π bonds
θ_m	Deformed bond-angle m
Θ_m	Equilibrium bond-angle m
ρ_m	Deformed bond length of bond m
ρ_m	Equilibrium bond length of bond m

Truss and continuum models

a	Elastic rod type of outer portion of truss representative volume element
A_m^n	Cross-sectional area of rod m of truss member type n
A^{nt}	Cross-sectional area of carbon nanotube
b	Elastic rod type of inner portion of truss representative volume element
D	Bending rigidity of a continuum plate
I	Moment of inertia of a continuum plate
r_m^n	Deformed distance between joints of rod m of truss member type n
R_m^n	Undeformed distance between joints of rod m of truss member type n
t	Thickness of a continuum plate (wall thickness of continuum tube)
Y^{g}	Young's modulus of graphene sheet
Y_m^n	Young's modulus of rod m of truss member type n
Y^{nt}	Young's modulus of carbon nanotube
r^{c}	Mid-plane radius of continuum nanotube wall
r_i^c	Inner radius of continuum nanotube wall
r_o^c	Outer radius of continuum nanotube wall
Λ^{c}	Mechanical strain energy of the continuum model
Λ^{t}	Mechanical strain energy of the truss model
ν	Poisson's ratio of graphene sheet

Boundary conditions

u_i	Displacement components of equivalent-continuum representative volume element
x_i	Cartesian coordinate system of the representative volume element
ε_{ij}	Strain components in the equivalent-continuum representative volume element
ε	Applied strain
γ	Applied shear strain

corresponding bulk properties of the material at the macroscopic scale. The advantages of the proposed method are its simplicity and direct connection with computational chemistry and solid mechanics.

In addition, the proposed method has been demonstrated with two independent examples that have direct application to the development and characterization of single-walled carbon nanotubes (SWNT). First, the effective geometry of a graphene sheet has been determined. A representative volume element (RVE) of the graphene layer has been modeled as a continuous plate with an effective thickness that has been determined from the bulk in-plane properties of graphite [2]. Second, the effective bending rigidity of a graphene sheet has been determined. The bending rigidity of the elastic plate has been described in terms of the atomic interactions that dominate the overall bending behavior.

2. Carbon nanotubes

In 1991 Iijima [3] obtained transmission electron micrographs of elongated, nano-sized carbon particles that consisted of cylindrical graphitic layers, known today as carbon nanotubes (Fig. 1). Since then, carbon nanotubes have become a primary focus in nanotechnology research due to their apparent exceptionally high stiffness and strength [1]. One of the fundamental issues that scientists and engineers are confronting is the characterization of the mechanical behavior of individual

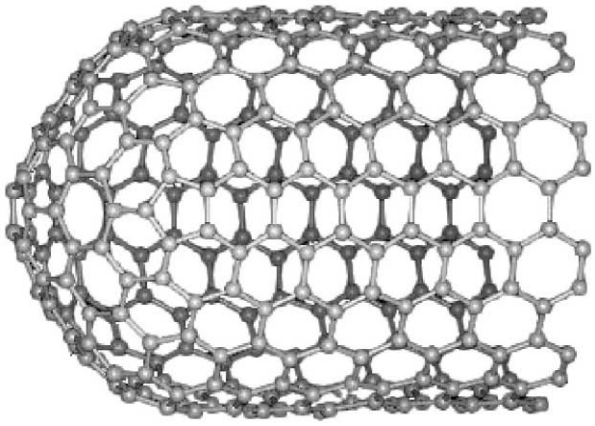

Fig. 1. End section of a single-walled carbon nanotube.

carbon nanotubes. Two independent components of this issue, the wall thickness and bending rigidity of carbon nanotubes, are discussed below.

2.1. Wall thickness

Many experimental [4–8] and theoretical [9–14] studies have been performed on single- and multi-walled carbon nanotubes. In particular, deformation modes and nanotube stiffnesses have been closely examined.

Physical properties, such as effective cross-sectional area and moment of inertia, and mechanical properties, such as Young's modulus and Poisson's ratio, are traditionally associated with the macroscopic-length scale, where the characteristic dimensions of a continuum solid are well defined. The determination of these properties has been attempted in many of the studies cited above without proper regard to an acceptable definition of the nanotube geometry. Accurate values of macroscopic physical and mechanical properties are crucial in establishing a meaningful link between nanotube properties and the properties of larger structures, such as nanotube-reinforced polymer composites. Therefore, caution should be used when applying continuum-type properties to nano-structured materials.

In many studies, it has been assumed that the nanotube "wall thickness" is merely the inter-planar spacing of two or more graphene sheets [5,8–13], which is about 0.34 nm in single-crystal graphite. While this simple idealization appears to have intuitive merit, it does not necessarily reflect the *effective* thickness that is representative of continuum properties. In order to avoid this problem, Hernandez et al. [10] proposed the use of a specific Young's modulus, i.e., Young's modulus per unit thickness. Even though this approach is convenient for studies concerned with the relative stiffnesses of nanotubes, it is of little use when modeling a nanotube as a continuum structure. Another proposed solution to this dilemma is to assume that the nanotube is a solid cylinder [15,16]. This method is certainly convenient, however, significant inconsistencies arise when comparing moduli data of single wall nanotubes (SWNT) and multi-walled nanotubes (MWNT) when both are assumed to be solid cylinders.

It follows that in order to properly model the mechanical behavior of a SWNT using continuum mechanics, the effective geometry must be known. If the nanotube is modeled as a continuous hollow cylinder with an effective wall thickness, then a simple first step is to model the flat graphene sheet in order to determine the effective wall thickness. In the current study, the effective thickness will be calculated as an example of the proposed modeling approach.

2.2. Bending rigidity

Due to the aspect ratio and tube-like geometry of SWNT, many studies have been conducted concerning the buckling and bending response of nanotubes using both theoretical [12,15,17–20] and experimental [21,22] approaches. In particular, Overney et al. [17] conducted a computational study and calculated a bending parameter of a graphene sheet based on the vibrational modes of a nanotube. Yakobson et al. [18] used computational methods to study the buckling of carbon nanotubes. They modeled the nanotubes as shells with a bending rigidity proportional to the Young's modulus and shell-wall thickness. Using the computationally obtained bending parameters, they calculated the Young's modulus and wall thickness of the shell. Govindjee and Sackman [19] theoretically investigated the validity of continuum mechanics at the nano-scale by examining the bending of multi-walled carbon nanotubes. They also assumed that the bending rigidity of each layer is proportional to the Young's modulus and moment of inertia. In each of these studies it is clear that the bending and buckling behavior of carbon nanotubes is highly dependent on the bending properties of the graphene sheet. Therefore, it follows that the bending behavior of a graphene sheet must be well-understood, and should be described in terms of the atomic properties of graphene.

According to the classical elasticity theory, it is assumed that the bending rigidity, D, of an isotropic solid is related to the cross-sectional geometry and the in-plane modulus [23]:

$$D = \frac{Y^{g} t^{3}}{12(1-\nu^{2})} \tag{1}$$

and

$$D = Y^{g} I \tag{2}$$

which are for the bending of plates and beams, respectively. In Eqs. (1) and (2), Y^{g}, ν, I, and t are the Young's

modulus, Poisson's ratio, moment of inertia, and plate thickness of a graphene sheet, respectively. It seems logical that these equations could describe the bending properties of graphene sheets and nanotubes due to geometric similarities to solid plates and/or beams. However, Ru [20] has pointed out that a discrepancy exists in the use of Eq. (1) when describing bending properties of carbon nanotubes. If the bending rigidity described by this equation is used in the bending analysis of carbon nanotubes, then an equivalent wall thickness must be used that is very small compared to the inter-planar spacing of graphene sheets. For example, Yakobson et al. [18] showed that the bending rigidity of carbon nanotubes is much smaller than that described by Eq. (1) if the typically assumed effective thickness of 0.34 nm (the inter-plane spacing of layers of graphite) of graphene sheets is used. They derived an effective thickness and Young's modulus of 0.066 nm and 5.5 Tpa, respectively, for a SWNT. The argument of Ru [20] is further supported by examining the chemical structure of a graphene sheet. At first glance, it appears that a graphene sheet would have very little bending rigidity since the atomic C–C bonds lie very close to the neutral axis during cylindrical bending, unlike continuous elastic plates in which there is material that is not on the neutral axis that contributes a resistance in bending that is proportional to the in-plane Young's modulus [Eqs. (1) and (2)]. Therefore, the primary atomic bonds, which are the main contribution to the in-plane elastic properties of graphene, should provide little, perhaps negligible, contribution to the bending rigidity of graphene sheets. The resistance to bending must be due to a different atomic interaction, which is discussed in Section 5.

3. Modeling procedure

The proposed method of modeling nano-structured materials with an equivalent-continuum is outlined below. Since the approach uses the energy terms that are associated with molecular mechanics modeling, a brief description of molecular mechanics is given first followed by an outline of the equivalent-truss and equivalent-continuum model development.

3.1. Molecular mechanics

An important component in molecular mechanics calculations of the nano-structure of a material is the description of the forces between individual atoms. This description is characterized by a force field. In the most general form, the total molecular potential energy, E^{nsm}, for a nano-structured material is described by the sum of many individual energy contributions:

$$E^{\text{nsm}} = \sum E^{\rho} + \sum E^{\theta} + \sum E^{\tau} + \sum E^{\omega} + \sum E^{\text{vdW}} + \sum E^{\text{el}} \tag{3}$$

where E^{ρ}, E^{θ}, E^{τ}, and E^{ω} are the energies associated with bond stretching, angle variation, torsion, and inversion, respectively (the reader should refer to a molecular mechanics text, e.g. [24], for a detailed description of these energy terms). The nonbonded interaction energies consist of van der Waals, E^{vdW}, and electrostatic, E^{el}, terms. The summation occurs over all of the corresponding interactions in the considered volume of the nano-structured material. Various functional forms may be used for these energy terms depending on the particular material and loading conditions considered [24]. Obtaining accurate parameters for a force field amounts to fitting a set of experimental or calculated data to the assumed functional form, specifically, the force constants and equilibrium structure. In situations where experimental data are either unavailable or very difficult to measure, quantum mechanical calculations can be a source of information for defining the force field.

3.2. Truss model

In order to simplify the calculation of the total molecular potential energy of molecular models with complex molecular structures and loading conditions, an intermediate model may be used to substitute for the molecular model. Due to the nature of molecular force fields, a pin-jointed truss model may be used to represent the energies given by Eq. (3), where each truss member represents the forces between two atoms. Therefore, a truss model allows the mechanical behavior of the nano-structured system to be accurately modeled in terms of displacements of the atoms. This mechanical representation of the lattice behavior serves as an intermediate step in linking the molecular potential with an equivalent-continuum model. In the truss model, each truss element corresponds to a chemical bond or a significant non-bonded interaction. The stretching potential of each bond corresponds with the stretching of the corresponding truss element. Traditionally, atoms in a lattice have been viewed as masses that are held in place with atomic forces that resemble elastic springs [25]. Therefore, bending of truss elements is not needed to simulate the chemical bonds, and it is assumed that each truss joint is pinned, not fixed.

The mechanical strain energy, Λ^t, of the truss model is expressed in the form:

$$\Lambda^t = \sum_n \sum_m \frac{A_m^n Y_m^n}{2R_m^n} \left(r_m^n - R_m^n\right)^2 \tag{4}$$

where A_m^n and Y_m^n are the cross-sectional area and Young's modulus, respectively, of rod m of truss member type n. The term $\left(r_m^n - R_m^n\right)$ is the stretching of rod m of truss member type n, where R_m^n and r_m^n are the undeformed and deformed lengths of the truss elements, respectively.

In order to represent the chemical behavior with the truss model, Eq. (4) must be equated with Eq. (3) in a physically meaningful manner. Each of the two equations are sums of energies for particular degrees of freedom. The main difficulty in the substitution is specifying Eq. (4), which has stretching terms only, for Eq. (3), which also has bond-angle variance and torsion terms. No generalization can be made for overcoming this difficulty for every nano-structured system. A feasible solution must be determined for a specific nano-structured material depending on the geometry, loading conditions, and degree of accuracy sought in the model.

3.3. Equivalent-continuum model

For many years, researchers have developed methods of modeling large-area truss structures with equivalent-continuum models [26–31]. These studies indicate that various methods and assumptions have been employed in which equivalent-continuum models have been developed that adequately represent truss structures. In general, the equivalent-continuum model is defined as a continuum that has the following characteristics:

1. Truss lattices with pinned joints are modeled as classical continua where micropolar [32] continuum assumptions are not necessary.
2. Local deformations are accounted for.
3. The temperature distribution, loading and boundary conditions of the continuum model simulate those of the truss model.
4. The same amount of thermoelastic strain energy is stored in the two models when deformed by identical static loading conditions.

The parameters of the equivalent-continuum model, such as the elastic properties and geometry, are determined based on the above characteristics. In some cases the strain energy of the continuum, Λ^c, can be easily formulated analytically and compared directly with Eq. (4) to obtain the equivalent-continuum properties. In other cases, especially with complex geometries and deformations, numerical tools need to be used to determine the continuum parameters. Once the properties of the equivalent-continuum model have been determined, the mechanical behavior of larger structures consisting of the nano-structured material may be predicted using the standard tools of continuum mechanics.

4. Example 1: effective geometry of a graphene sheet

In this section, a graphene sheet is modeled as a continuous plate with a finite thickness that represents the effective thickness for the determination of continuum-type mechanical and physical properties. By using the methodology described above, the molecular mechanics model is substituted with a truss model and subsequently an equivalent-plate model. The continuum model may then be used in further solid mechanics-based analyses of SWNT.

4.1. Representative volume element

To reduce the computational time associated with modeling the graphene sheet, a representative volume element (RVE) for graphene was used in this study (Fig. 2). The selected RVE allows each degree of freedom of the carbon atom associated with bond stretching and bond-angle variation in the hexagonal ring to be completely modeled by truss and continuum finite element model nodal-displacement degrees of freedom. Also, this RVE allows the displacements on the boundary of the proposed chemical, truss, and continuum models to correspond exactly. Furthermore, macroscopic loading conditions applied to a continuous graphene plate can be easily reduced to periodic boundary conditions that are applied to the RVE.

4.2. Molecular mechanics model

The specific forms of the energy terms in Eq. (3) used in this example were taken from the AMBER force field of Kollman and coworkers [33,34]. Due to the nature of the material and loading conditions in the present study, only the bond stretching and bond-angle variation energies were included. Torsion, inversion, and non-bonded interactions were assumed to be negligible for the case of a graphene lattice subjected to small deformations. For this example, the molecular potential energy of a graphene sheet with carbon-to-carbon bonds is expressed as a sum of simple harmonic functions:

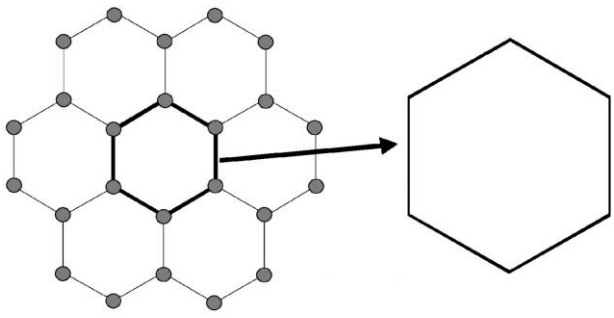

Fig. 2. Representative volume element of a graphene sheet.

$$E^{g} = \sum_{m} K_m^{\rho}(\rho_m - \rho_m)^2 + \sum_{m} K_m^{\theta}(\theta_m - \Theta_m)^2 \tag{5}$$

where the terms ρ_m and Θ_m refer to the undeformed interatomic distance of bond m and the undeformed bond-angle m, respectively. The quantities ρ_m and θ_m are the bond length and angle after stretching, respectively (see Fig. 3). K_m^{ρ} and K_m^{θ} are the force constants associated with the stretching and angle variance of bond and bond-angle m, respectively. Using the parameters for the AMBER force field [33], the force constants used in this example are:

$$K^{\rho} = 46900\frac{\text{kcal}}{\text{mol}\cdot\text{nm}^2} = 3.26\cdot10^{-7}\frac{\text{nJ}}{\text{bond}\cdot\text{nm}^2}$$
$$K^{\theta} = 63\frac{\text{kcal}}{\text{mol}\cdot\text{rad}^2} = 4.38\cdot10^{-10}\frac{\text{nJ}}{\text{angle}\cdot\text{rad}^2} \tag{6}$$

The equilibrium bond length, ρ_m, is 0.140 nm, and the undeformed bond-angle, Θ_m, is 120.0°.

4.3. Truss model

In order to express the mechanical strain energy, Λ^t, of the truss model in terms of the variable truss joint angles that are specified in molecular mechanics ($\theta_m - \Theta_m$), the RVE has been modeled with additional rods between nearly adjacent joints to represent the interaction between the corresponding carbon atoms (Fig. 3). In order to represent the chemical model, which has bond stretching and variable angles as degrees of freedom, with a truss model that has stretching degrees of freedom only, two types of elastic rods, a and b, are incorporated into the truss RVE. Alternatively, a torsional spring element may be used to model the bond-angle variation, however, the number of degrees of freedom of every truss joint (and the complexity of the model) is significantly increased.

The mechanical strain energy, Λ^t, of the discrete truss system shown in Fig. 3 is expressed in the form of Eq. (4) as:

$$\Lambda^t = \sum_{m} \frac{A_m^a Y_m^a}{2R_m^a}\left(r_m^a - R_m^a\right)^2 + \sum_{m} \frac{A_m^b Y_m^b}{2R_m^b}\left(r_m^b - R_m^b\right)^2 \tag{7}$$

where the superscripts correspond to rod types a and b, respectively. Comparing Eqs. (5) and (7), it is clear that the bond stretching term in the Eq. (5) can be related to the first term of Eq. (7) for the rods of type a:

$$K_m^{\rho} = \frac{A_m^a Y_m^a}{2R_m^a} \tag{8}$$

where it is assumed that $\rho_m = r_m^a$ and $\rho_m = R_m^a$. However, the second terms in Eqs. (5) and (7) cannot be related directly. In order to equate the constants, the chemical bond-angle variation must be expressed in terms of the elastic stretching of the truss elements of type b. For simplicity, it may be assumed that the prescribed loading conditions consist of small, elastic deformations only, even though, in general, the proposed modeling approach could be applied to larger deformations. This assumption is not an over-simplification for the graphene sheet since the deformations for highly stiff linear-elastic materials subjected to many practical loading conditions are quite small.

In order to express the Young's modulus of the rods of type b in terms of the bond-angle force constant, a relationship between the change in the bond angle and the corresponding change in length of the type b truss element is required. If it is assumed that the changes in bond angle are small, then it can be easily shown that (see Fig. 4):

$$\theta_m - \Theta_m \approx \frac{2\left(r_m^b - R_m^b\right)}{R_m^a} \tag{9}$$

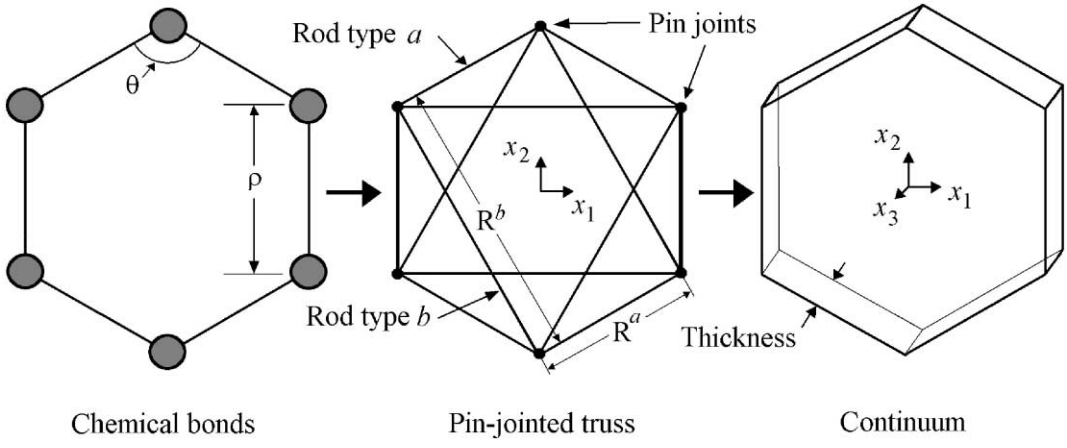

Fig. 3. Representative volume elements for the chemical, truss, and continuum models.

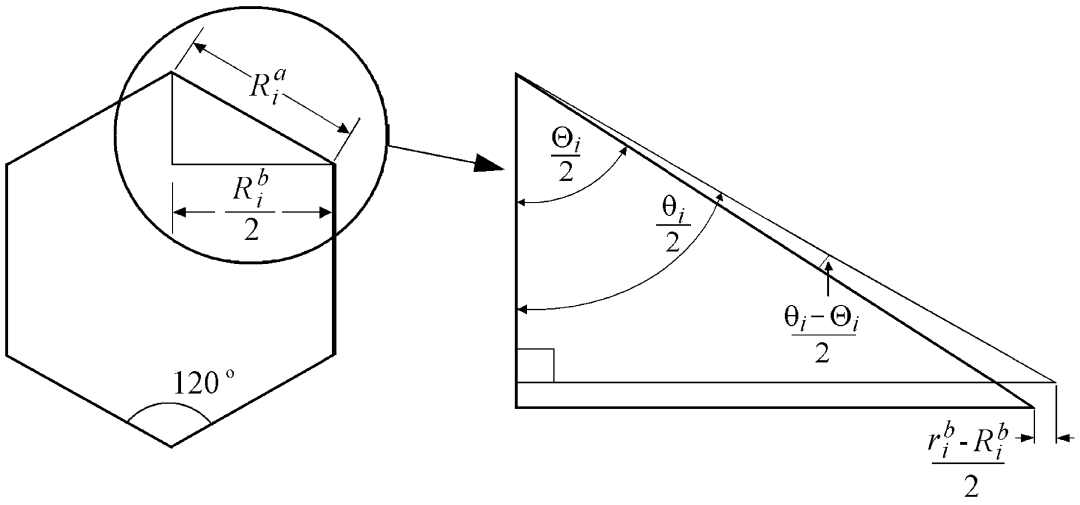

Fig. 4. Schematic of the deformed geometry of the representative volume element.

The right-hand side of Eq. (9) is four times larger than the right hand side of Eq. (8) given by Odegard et al. [35]. This discrepancy is due to an improvement in the assumptions used to derive Eq. (9) in the current study. Substitution of Eq. (9) into Eqs. (5) and (7) results in the following approximation:

$$K_m^\theta = \frac{R_m^b A_m^b Y_m^b}{24} \tag{10}$$

Therefore, the Young's moduli of the two rod types are:

$$\begin{aligned} Y_m^a &= \frac{2K_m^\rho R_m^a}{A_m^a} \\ Y_m^b &= \frac{24K_m^\theta}{R_m^b A_m^b} \end{aligned} \tag{11}$$

The strain energy of the truss model may then be expressed in terms of the force constants:

$$\Lambda^t = \sum_m K^\rho \left(r_m^a - R_m^a\right)^2 + \sum_m \frac{12K^\theta}{\left(R_m^b\right)^2}\left(r_m^b - R_m^b\right)^2 \tag{12}$$

4.4. Equivalent-plate model

Working with the assumptions discussed herein, the next step in linking the molecular and continuum models is to replace the equivalent-truss model with an equivalent-continuous plate with a finite thickness (Fig. 3). For this example, it is assumed that the truss and continuum models are equivalent when the elastic strain energy stored in the two models are equal under identical displacement boundary conditions. The value of the plate thickness that results in equal strain energies is the assumed effective thickness of the graphene sheet.

While the mechanical properties of the truss elements have been determined as described above, those of the graphene sheet were taken from the literature. Values for the in-plane mechanical properties of graphite have been measured macroscopically, i.e., without any assumptions regarding the graphene sheet thickness. For this example, the values of the Young's modulus and Poisson's ratio of bulk graphite are $Y^g = 1008$ GPa and $\nu = 0.145$, respectively [2]. For simplicity, it is assumed that graphite is isotropic since no out-of-plane deformations are considered here. Given that there are no consistent data available on the properties of a single graphene sheet, these properties of the graphene sheet are based on the in-plane properties of bulk graphite.

4.5. Boundary conditions

In order to determine an effective plate thickness, both the truss and continuum models were subjected to three sets of loading conditions. For each set of loading conditions, a corresponding effective thickness was determined. The loading conditions correspond to the three fundamental in-plane deformations of a plate, that is, uniform axial tension along x_1 and x_2 and pure shear loading in the x_1 and x_2 plane.

For a uniaxial deformation along the x_2 direction (load case I), the RVE may be subjected to the following boundary conditions (Fig. 5) [35]:

$$\begin{aligned} u_1 &= -\nu\varepsilon x_1 \\ u_2 &= \varepsilon x_2 \\ u_3 &= -\nu\varepsilon x_3 \end{aligned} \tag{13}$$

where the displacement components are parallel to the corresponding RVE coordinates. The total strain energy can be calculated using [23]:

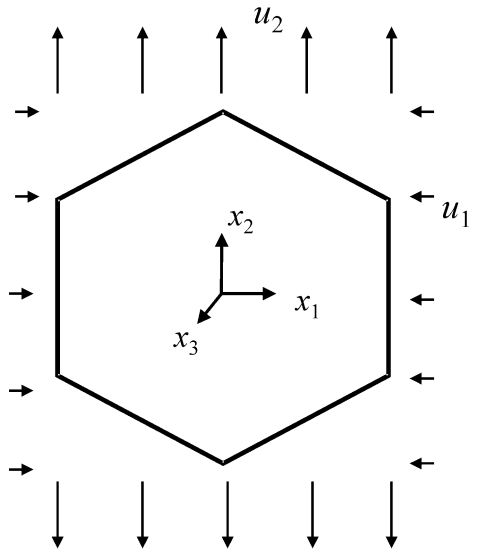

Fig. 5. Load case I: extension along x_2.

$$\Lambda^c = \frac{VY^g}{2(1+\nu)}\left[\frac{\nu}{1-2\nu}\varepsilon_{kk}^2 + \varepsilon_{ij}\varepsilon_{ij}\right] \tag{14}$$

where V is the volume of the RVE, $i,j,k = 1,2,3$ (using summation notation), and the components of the strain tensor, ε_{ij}, are given by:

$$\varepsilon_{ij} = \frac{1}{2}\left(\frac{\partial u_j}{\partial x_i} + \frac{\partial u_i}{\partial x_j}\right) \tag{15}$$

For the RVE under the conditions given in Eq. (13):

$$\Lambda^c = \frac{3\sqrt{3}}{4}(R^a)^2 t Y^g \varepsilon^2 \tag{16}$$

where t is the thickness of the continuum plate. For a uniaxial deformation along the x_1 direction (load case II), the boundary conditions are (Fig. 6) [35]:

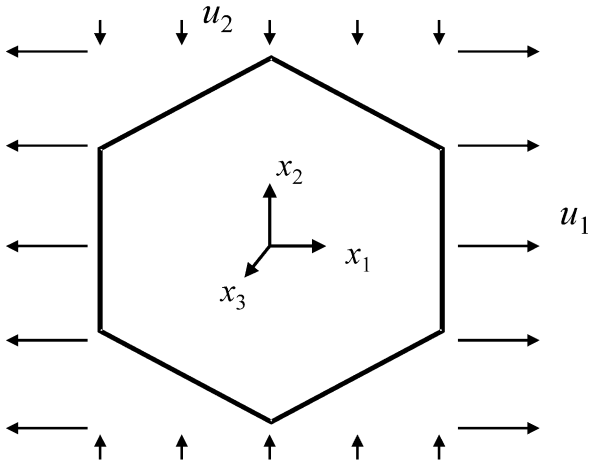

Fig. 6. Load case II: extension along x_1.

$$\begin{aligned} u_1 &= \varepsilon x_1 \\ u_2 &= -\nu\varepsilon x_2 \\ u_3 &= -\nu\varepsilon x_3 \end{aligned} \tag{17}$$

The total strain energy of an equivalent-continuum RVE under this condition is given by Eq. (16). For a pure shear strain in the x_1-x_2 plane (Load case III), the RVE may be subjected to the following boundary conditions (Fig. 7) [35]:

$$\begin{aligned} u_1 &= 0 \\ u_2 &= \gamma x_1 \\ u_3 &= 0 \end{aligned} \tag{18}$$

The total strain energy of an equivalent-continuum RVE under this condition is:

$$\Lambda^c = \frac{3\sqrt{3}}{8}(R^a)^2 t \frac{Y^g}{(1+\nu)}\gamma^2 \tag{19}$$

4.6. Results and discussion

The strain energy of the truss model was calculated using a finite element analysis (ANSYS 5.7®) for all three boundary conditions. The strain energies of each truss element were summed to obtain the total strain energy for the RVE. The resulting strain energy was equated with Eq. (16) or (19) for Load cases I and II or

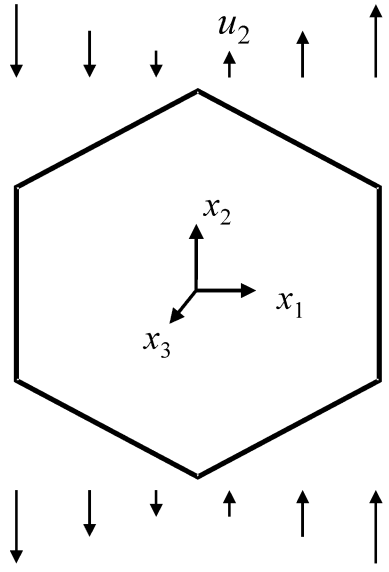

Fig. 7. Load case III: pure shear.

III, respectively, and the corresponding effective thickness of the equivalent-continuum plate, t, was determined. Each extensible rod was modeled using a finite truss element (LINK1) with two degrees of freedom at each node (displacements parallel to x_1 and x_2). The cross-sectional areas of the type a rods were divided by a factor of 2, since these rods are sharing their total area with adjacent RVEs. For Load cases I and II, the resulting effective thickness was calculated to be 0.69 nm. For Load case III, the effective thickness was 0.57 nm. These values are significantly larger than the widely accepted value for the graphitic inter-planar spacing, 0.34 nm, and much larger than the value suggested by Yakobson et al. [18] of 0.066 nm.

It may be assumed that during uniaxial loading of a carbon nanotube, with the force and strain known, the Young's modulus can be calculated using:

$$Y^{\mathrm{nt}} \propto \left(A^{\mathrm{nt}}\right)^{-1} \tag{20}$$

where A^{nt} is the cross-sectional area of the hollow continuum cylinder with a constant mid-plane radius, r^{c}. The inner radius, $r_{\mathrm{i}}^{\mathrm{c}}$, and outer radius, $r_{\mathrm{o}}^{\mathrm{c}}$, of the tube are (Fig. 8):

$$\begin{aligned} r_{\mathrm{i}}^{\mathrm{c}} &= r^{\mathrm{c}} - \frac{t}{2} \\ r_{\mathrm{o}}^{\mathrm{c}} &= r^{\mathrm{c}} + \frac{t}{2} \end{aligned} \tag{21}$$

where $r^{\mathrm{c}} \geqslant t/2$. The cross-sectional area of the hollow continuum cylinder is:

$$A^{\mathrm{nt}} = 2\pi t r^{\mathrm{c}} \tag{22}$$

The calculated cross-sectional areas using the effective thickness values obtained above are shown in Table 1. The ratios of the calculated Young's modulus based on the effective thickness obtained for the three load cases, their average, and from Yakobson et al. [18], to the Young's modulus based on inter-planar spacing, are also provided in Table 1. It was assumed that the mechanical properties of the SWNT wall are equal to those of the equivalent-plate model. The results shown in Table 1 suggest that measured and calculated values of mechanical properties of carbon nanotubes that are dependent on the dimensions of the continuum tube may differ significantly based on the assumed geometry.

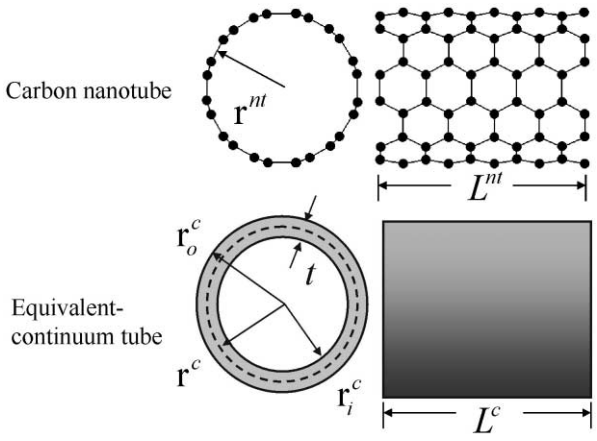

Fig. 8. Geometry of a carbon nanotube and an equivalent-continuum tube.

5. Example 2: effective bending rigidity of a graphene sheet

In this section, a graphene sheet is again modeled as a continuous plate. The bending rigidity of the plate is assumed to be independent of the in-plane mechanical properties and thickness of the plate. By using the proposed modeling method, the molecular mechanics model is used to determine the effective bending rigidity of the continuum plate.

5.1. Molecular mechanics model

It has been shown that the only significant change in the electronic structure of a flat graphene sheet when subjected to pure bending is the change in the π-orbital electron density on either side of the graphene sheet (i.e. inversion, see Fig. 9) [36–41]. This indicates that the inversion alone contributes to the bending resistance of graphene sheets. Bakowies and Theil [36] have suggested that the increase in the total molecular potential energy per carbon atom of a carbon cluster (i.e. a structure formed by a single plane of carbon atoms, such as carbon Fullerenes and SWNT) with respect to a flat graphene sheet may be closely approximated as:

$$E^{\omega} = K^{\omega}\bar{\phi}_p^2 \tag{23}$$

where K^{ω} is a force constant and $\bar{\phi}_p$ is the average inversion angle defined as (in radians):

Table 1
Ratio of calculated Young's modulus for different wall thicknesses of SWNT with respect to the Young's modulus calculated with the inter-planar spacing

	Continuum wall thickness (nm)	Continuum cross-sectional area (nm^2)	Ratio of Young's moduli
Load cases I and II	0.69	$4.34r^{\mathrm{c}}$	0.49
Load case III	0.57	$3.58r^{\mathrm{c}}$	0.60
Average of I, II and III	0.65	$4.08r^{\mathrm{c}}$	0.52
Yakobson et al. (1996)	0.07	$0.44r^{\mathrm{c}}$	4.86
Inter-planar spacing	0.34	$2.14r^{\mathrm{c}}$	1.00

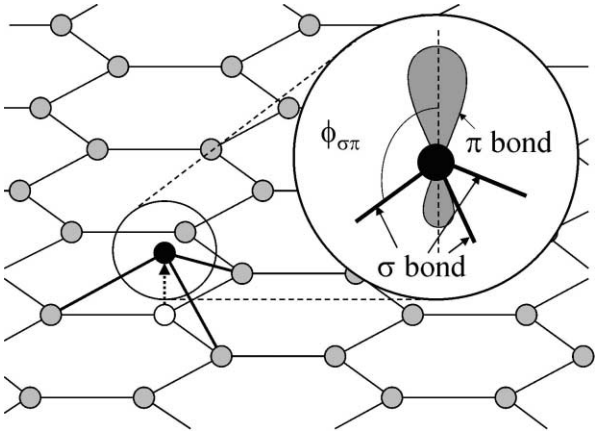

Fig. 9. Bond inversion of carbon atom in a graphene sheet.

$$\bar{\phi}_p = \frac{\sum_p \left(\phi_{\sigma\pi} - \frac{\pi}{2}\right)}{p} \tag{24}$$

where p is the total number of carbon atoms in the carbon structure considered and $\phi_{\sigma\pi}$ is the angle defined in Fig. 9. For simplicity in the specific case of carbon nanotubes, the π-orbital axis vector technique [42] can be used to show that the change in the molecular potential energy due to inversion can be expressed in terms of the nanotube radius, r^{nt}:

$$E^{\omega} = \frac{\overline{K^{\omega}}}{(r^{\mathrm{nt}})^2} \tag{25}$$

where $\overline{K^{\omega}}$ is a modified inversion force constant given by:

$$\overline{K^{\omega}} = \left(0.0012 \ \mathrm{rad^2 nm^2}\right) K^{\omega} \tag{26}$$

Values of the force constant, $\overline{K^{\omega}}$, have been determined using computational chemistry data from several studies [36,43–46] and Eq. (25). Even though the computational chemistry data was obtained for the specific case of bending of graphene sheets to form complete nanotubes or nanotube-like structures, the concepts of structural mechanics can be implemented such that these values could apply to any bending mode of graphene sheets. The values are shown in Table 2 along with the overall average, which is:

$$\overline{K^{\omega}} = 0.018 \ \frac{\mathrm{eV \cdot nm^2}}{\mathrm{atom}} \tag{27}$$

The total number of carbon atoms per nanotube is [43]:

$$N = \frac{4\pi r^{\mathrm{nt}} L^{\mathrm{nt}}}{3\alpha^2} \tag{28}$$

Table 2
Values of force constant associated with bond inversion of graphene sheet

Study	$\overline{K^{\omega}}$ (eV×nm^2/atom)
Bakowies and Thiel [36]	0.016
Robertson et al.—EP1 [43]	0.016
Robertson et al.—EP2 [43]	0.011
Robertson et al.—LDF [43]	0.021
Sawada and Hamada [44]	0.017
Miyamoto et al. [45]	0.020
Hernandez et al. (*n*,*n*) [46]	0.021
Hernandez et al. (*n*,0) [46]	0.022
Average	0.018

where α is the interatomic spacing of carbon atoms and L^{nt} is the nanotube length. Therefore, the total change in the molecular potential energy of a nanotube due to inversion is:

$$E^{\omega} N = \frac{4\pi L^{\mathrm{nt}} \overline{K^{\omega}}}{3\alpha^2 r^{\mathrm{nt}}} \tag{29}$$

5.2. Equivalent-continuum plate

In the case of a graphene sheet subjected to pure bending, the total molecular potential energy is easily described with a single force constant by using Eq. (29), unlike the example discussed in the previous section where an intermediate truss model was needed in order to calculate the strain energy under various loading conditions. Therefore, the truss model is not needed in this particular example and an equivalent-continuum model has been developed by equating the total molecular potential energy of the molecular model and the strain energy of the continuum plate directly.

The strain energy of a plate of length L^{c} subjected to cylindrical curvature (Fig. 8) is [47]:

$$\Lambda^{\mathrm{c}} = \frac{\pi D L^{\mathrm{c}}}{r^{\mathrm{c}}} \tag{30}$$

where r^{c} is the radius of curvature, D is the bending rigidity, and the superscript c denotes the strain energy associated with the continuum plate. In this case, D is not defined by Eqs. (1) or (2) for the reasons discussed above. In order to determine the bending rigidity of the equivalent-continuum plate that represents the actual effective bending rigidity of the graphene sheet, the strain energy of the continuum plate and the increase in the total molecular potential energy of the graphene sheet must be equivalent when subjected to pure bending. Equating Eqs. (29) and (30) results in:

$$D = \frac{4\overline{K^{\omega}}}{3\alpha^2} \tag{31}$$

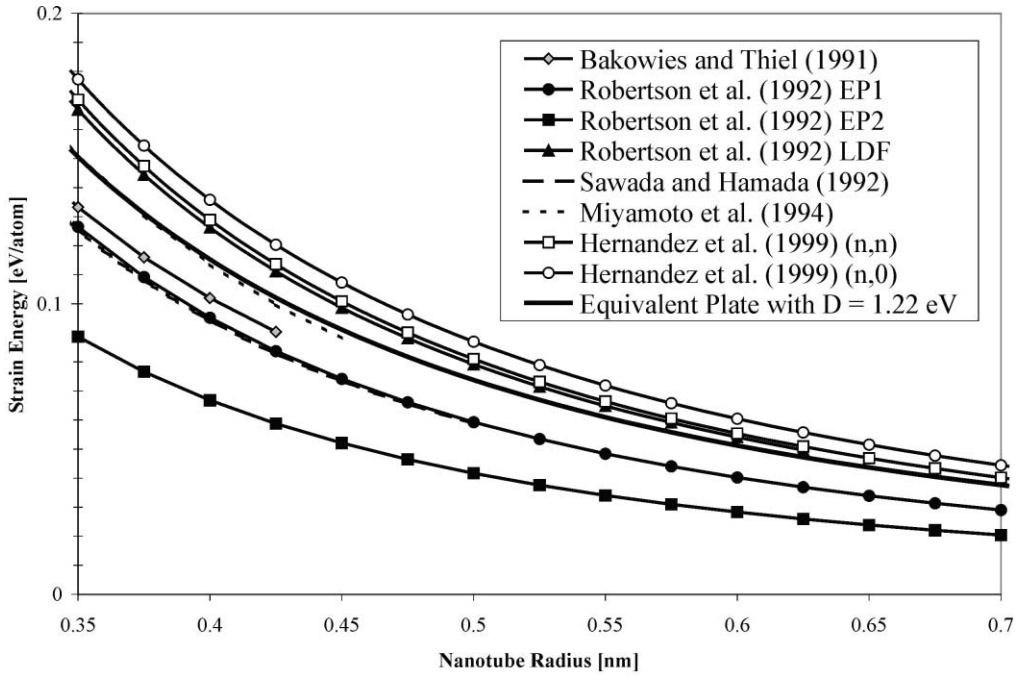

Fig. 10. Strain energy of a graphene sheet subjected to cylindrical bending.

Therefore, the effective bending rigidity is directly proportional to the inversion force constant and the inverse square of the interatomic spacing of graphite.

The equivalent bending rigidity for the equivalent-continuum plate is calculated using Eq. (31) and the average value of the force constant $\overline{K^{\omega}}$, given in Table 2, and with $\alpha = 0.140$ nm [2] to give $D = 1.22$ eV. This value is 44% higher than that used by Yakobson et al. [18] and Robertson et al. [43] ($D = 0.85$ eV).

The strain energy of a graphene sheet is presented in Fig. 10 for different nanotube radii for all of the computational chemistry data and the equivalent continuum plate model. It is assumed that the graphene sheet behaves elastically in bending for all nanotube radii. Clearly, the trends of the computational chemistry data and the equivalent-continuum model are in agreement.

6. Summary

A method has been presented for modeling structure-property relationships of nano-structured materials. This method serves to link computational chemistry, which is used to predict molecular properties, and solid mechanics, which describes macroscopic mechanical behavior based on bulk material properties. This link is established by replacing discrete molecular structures with equivalent-continuum models. It has been shown that this replacement may be accomplished by equating the molecular potential energy of nano-structured materials with the mechanical strain energy of a representative continuum model. The development of an equivalent-truss model may be used as an intermediate step in establishing the equivalent-continuum model.

The proposed modeling method has been applied to determine the effective geometry and effective bending rigidity of a graphene sheet. A representative volume element (RVE) of the chemical structure of a graphene sheet has been substituted with RVEs of equivalent-truss and equivalent-continuum models. As a result, an effective thickness of the continuum model has been determined. This effective thickness has been shown to be significantly larger than the inter-planar spacing of graphite. The effective bending rigidity of an equivalent-continuum plate model of a graphene sheet was also determined using the proposed method. The molecular potential energy of the molecular model of a graphene sheet subjected to cylindrical bending (to form a nanotube) was equated with the strain energy of an equivalent-continuum plate subjected to cylindrical bending.

Acknowledgements

This work was performed while Dr. Odegard and Dr. Wise held National Research Council Research Associateship Awards at NASA Langley Research Center.

References

[1] Edelstein AS, Cammarata RC. Nanomaterials: synthesis, properties and applications. Bristol: Institute of Physics Publishing; 1996.

[2] Kelly BT. Physics of graphite. Essex, England: Applied Science Publishers Ltd; 1981.

[3] Iijima S. Helical microtubules of graphitic carbon. Nature 1991; 354:56–8.

[4] Treacy MMJ, Ebbesen TW, Gibson JM. Exceptionally high Young's modulus observed for individual carbon nanotubes. Nature 1996;381:678–80.

[5] Krishnan A, Dujardin E, Ebbesen TW, Yianilos PN, Treacy MMJ. Young's modulus of single-walled nanotubes. Physical Review B 1998;58(20):14013–9.

[6] Salvetat JP, Bonard JM, Thomson NH, Kulik AJ, Forro L, Benoit W, et al. Mechanical Properties of Carbon Nanotubes. Applied Physics A 1999;69:255–60.

[7] Yu M, Dyer MJ, Skidmore GD, Rohrs HW, Lu X, Ausman KD, et al. Three-dimensional manipulation of carbon nanotubes under a scanning electron microscope. Nanotechnology 1999;10: 244–52.

[8] Yu M, Lourie O, Dyer MJ, Moloni K, Kelly TF, Ruoff RS. Strength and breaking mechanism of multiwalled carbon nanotubes under tensile load. Science 2000;287:637–40.

[9] Lu JP. Elastic properties of carbon nanotubes and nanoropes. Physical Review Letters 1997;79(7):1297–300.

[10] Hernandez E, Goze C, Bernier P, Rubio A. Elastic properties of C and $B_xC_yN_z$ composite nanotubes. Physical Review Letters 1998;80(20):4502–5.

[11] Yao N, Lordi V. Young's modulus of single-walled carbon nanotubes. Journal of Applied Physics 1998;84(4):1939–43.

[12] Ozaki T, Iwasa Y, Mitani T. Stiffness of single-walled carbon nanotubes under large strain. Physical Review Letters 2000;84(8): 1712–5.

[13] Van Lier G, Van Alsenoy C, Van Doren V, Geerlings P. Ab initio study of the elastic properties of single-walled carbon nanotubes and graphene. Chemical Physics Letters 2000;326:181–5.

[14] Popov VN, Van Doren VE, Balkanski M. Elastic properties of crystals of single-walled carbon nanotubes. Solid State Communications 2000;114:395–9.

[15] Cornwell CF, Wille LT. Elastic properties of single-walled carbon nanotubes in compression. Solid State Communications 1997; 101(8):555–8.

[16] Wong EW, Sheehan PE, Leiber CM. Nanobeam mechanics: elasticity, strength, and toughness of nanorods and nanotubes. Science 1997;277:1971–5.

[17] Overney G, Zhong W, Tomanek D. Structural rigidity and low frequency vibrational modes of long carbon tubules. Zeitschrift Fur Physik D 1993;27:93–6.

[18] Yakobson BI, Brabec CJ, Bernholc J. Nanomechanics of carbon tubes: instabilities beyond linear response. Physical Review Letters 1996;76(14):2511–4.

[19] Govindjee S, Sackman JL. On the use of continuum mechanics to estimate the properties of nanotubes. Solid State Communications 1999;110:227–30.

[20] Ru CQ. Effective bending stiffness of carbon nanotubes. Physical Review B 2000;62(15):9973–6.

[21] Falvo MR, Clary GJ, Taylor RM, Chi V, Brooks FP, Washburn S, et al. Bending and buckling of carbon nanotubes under large strain. Nature 1997;389(6651):582–4.

[22] Lourie O, Cox DM, Wagner HD. Buckling and collapse of embedded carbon nanotubes. Physical Review Letters 1998;81(8): 1638–41.

[23] Timoshenko S, Goodier JN. Theory of elasticity. New York: McGraw-Hill Book Company; 1951.

[24] Rappe AK, Casewit CJ. Molecular mechanics across chemistry. Sausalito, California: University Science Books; 1997.

[25] Born M, Huang K. Dynamical theory of crystal lattices. London: Oxford University Press; 1954.

[26] Noor AK, Anderson MS, Greene WH. Continuum models for beam- and platelike lattice structures. AIAA Journal 1978;16(12): 1219–28.

[27] Sun C T, Kim B J, Bogdanoff J L. On the derivation of equivalent simple models for beam and plate-like structures in dynamic analysis. In: AIAA/ASME/ASCE/AHS 22nd structures, structural dynamics and materials conference. Atlanta, Georgia; 1981. p. 523–32.

[28] Noor AK. Continuum modeling for repetitive lattice structures. ASME Applied Mechanics Reveiws 1988;41(7):285–96.

[29] Dow JO, Huyer SA. Continuum models of space station structures. Journal of Aerospace Engineering 1989;2(4):220–38.

[30] Sun CT, Leibbe SW. Global–local approach to solving vibration of large truss structures. AIAA Journal 1990;28(2):303–8.

[31] Lee U. Equivalent continuum models of large plate-like lattice structures. International Journal of Solids and Structures 1994; 31(4):457–67.

[32] Eringen AC. Linear theory of micropolar elasticity. Journal of Mathematics and Mechanics 1966;15(6):909–23.

[33] Cornell WD, Cieplak P, Bayly CI, Gould IR, Merz KM, Ferguson DM, Spellmeyer DC, et al. A second generation force field for the simulation of proteins, nucleic acids, and organic molecules. Journal of the American Chemical Society 1995;117:5179–97.

[34] Weiner SJ, Kollman PA, Case DA, Singh UC, Ghio C, Alagona G, et al. A new force field for molecular mechanical simulation of nucleic acids and proteins. Journal of the American Chemical Society 1984;106:765–84.

[35] Odegard G M, Gates T S, Nicholson L M, Wise K E. Equivalent continuum modeling of nano-structured materials. NASA/TM-2001–210863; 2001.

[36] Bakowies D, Thiel W. MNDO Study of large carbon clusters. Journal of the American Chemical Society 1991;113:3704–14.

[37] Haddon RC. Chemistry of the fullerenes: the manifestation of strain in a class of continuous aromatic molecules. Science 1993; 261:1545–50.

[38] Blasé X, Benedict LX, Shirley EL, Louie SG. Hybridization effects and metallicity in small radius carbon nanotubes. Physical Review Letters 1994;72(12):1878–81.

[39] Rochefort A, Salahub DR, Avouris P. The effect of structural distortions on the electronic structure of carbon nanotubes. Chemical Physics Letters 1998;297:45–50.

[40] Chen Y, Haddon RC, Fang S, Rao AM, Eklund PC, Lee WH, et al. Chemical attachment of organic functional groups to single-walled carbon nanotube material. Journal of Materials Research 1998;13(9):2423–31.

[41] Srivastava D, Brenner DW, Schall JD, Ausman DD, Yu M, Ruoff RS. Predictions of enhanced chemical reactivity at regions of local conformational strain on carbon nanotubes: kinky chemistry. Journal of Physical Chemistry 1999;103:4330–7.

[42] Haddon RC. π-Electrons in three dimensions. Accounts of Chemical Research 1988;21:243–9.

[43] Robertson DH, Brenner DW, Mintmire JW. Energetics of nanoscale graphitic tubules. Physical Review B 1992;45(21): 12592–5.

[44] Sawada S, Hamada N. Energetics of carbon nano-tubes. Solid State Communications 1992;83(11):917–9.

[45] Miyamoto Y, Rubio A, Louie SG, Cohen ML. Electronic properties of tubule forms of hexagonal BC3. Physical Review B 1994; 50(24):18360–6.

[46] Hernandez E, Goze C, Bernier P, Rubio A. Elastic properties of single-wall nanotubes. Applied Physics A 1999;68:287–92.

[47] Timoshenko SP, Weinowsky-Kreiger S. Theory of plates and shells. New York: McGraw Hill; 1959.